$$E\left[\delta^r\right] = \frac{\sum_{k=1}^{N} \alpha_k \cdot \delta_{\alpha_k}^r}{N} \tag{4}$$

The mean and the standard deviation of the output fuzzy number can be computed with the first and second moments (r = 1 and 2).

CASE STUDY - TNEC EXCAVATION CASE

The TNEC excavation case in Taiwan (Ou et al., 1998) is used herein as an example to illustrate the *fuzzy finite element approach* (FFEA). To verify the accuracy of PLAXIS code with the MPP soil model, we re-analyze the case of the Taipei National Enterprise Center (TNEC). The results are compared with those reported previously by Kung et al. (2007). Fig. 2 compares the results of FEM predictions of the maximum wall deflections and the maximum ground settlements, respectively. The results show that the PLAXIS solutions in this paper are as accurate as those obtained by Kung et al. (2007) using AFENA and both agree well with field observations.

It is noted that the second layer (8 m – 33m) in the soil profile is a clay layer that dominates the maximum wall and ground responses in this excavation. For this case study of the TNEC excavation, the normalized undrained strength and the normalized initial tangent modulus of the clay are s_u/σ'_v = 0.32 and E_i/σ'_v = 672, respectively (Kung et al., 2007). Thus, the standard deviations of the two parameters are estimated to be 0.05 and 108, respectively, based on a reported coefficient of variation (COV) of 0.16 (Hsiao et al., 2008). The two soil parameters are treated here as triangular fuzzy numbers, since the available data is not sufficient to characterize them in term of probability distributions.

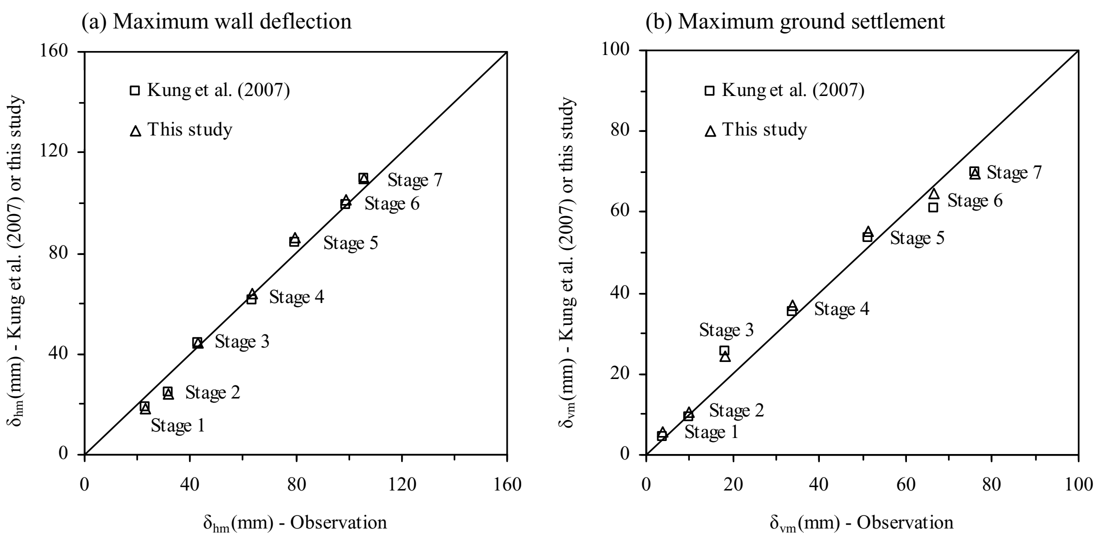

Figure 2. Maximum wall deflections and maximum ground settlements at various stages of excavation of the TNEC case.

To consider the effect of the spatial variability, let's *first* assume that the field has an infinite scale of fluctuation. The variance reduction factor (Γ^2) in this case is 1 (no reduction) and the fuzzy numbers for s_u/σ'_v and E_i/σ'_v can be constructed using the procedure described previously. Fig. 3 shows the constructed fuzzy numbers for s_u/σ'_v and E_i/σ'_v (note: the triangular membership function labeled *a-m-b* in this figure). All other input variables in the PLAXIS analysis are assumed to have non-random, non-fuzzy values. Analysis of the braced excavation in the TNEC case is carried out using PLAXIS with the MPP soil model. The resulting fuzzy numbers that represent the maximum wall deflection (δ_{hm}) and the ground-surface settlement (δ_{vm}) for the last excavation stage obtained from PLAXIS are shown in Fig. 4.

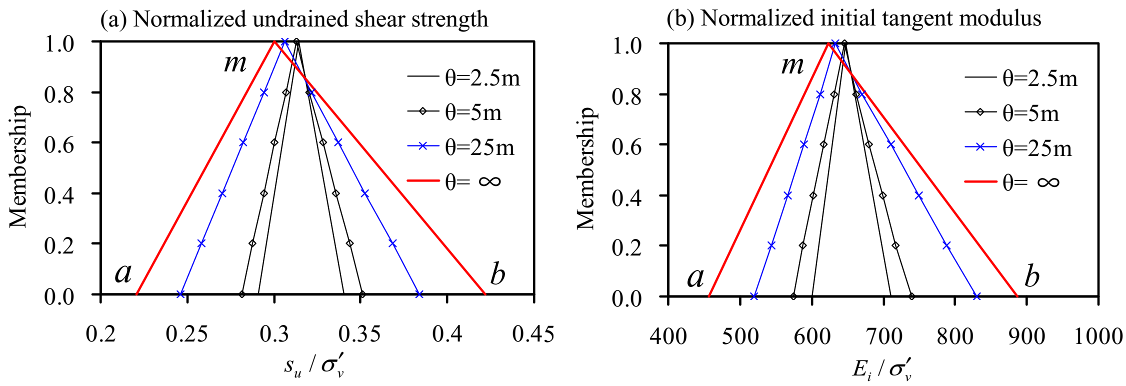

Figure 3. Fuzzy input parameters at different scales of fluctuation

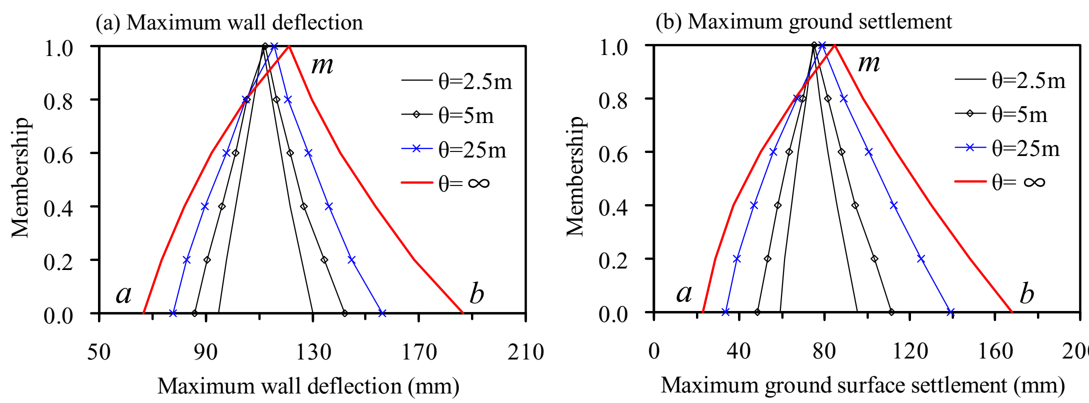

Figure 4. Resulting fuzzy numbers for maximum wall deflection and ground surface settlement

The entire processes of the above FFEA analysis can be repeated for any assumed scale of fluctuation. For simplicity and as an example here, the scales of fluctuation of the two soil parameters in this TNEC case are assumed to be the same; that is, $\theta = \theta_{s_u/\sigma'_v} = \theta_{E_i/\sigma'_v}$. For demonstration purposes and as a way to investigate the effect of spatial variability, the FFEA analysis is repeated for three additional scales of fluctuation (2.5m, 5m, and 25m). For each scenario involving a different scale of fluctuation, the variance reduction factor (Γ^2) is computed with Eq. (1) and the characteristic length L which is estimated to be 71 m in this case (the length of the sliding surface in this case). The constructed fuzzy numbers for these three scenarios are shown in Fig. 3. The resulting fuzzy numbers are also shown in Fig. 4.

For illustration purposes, the probabilities of exceedance are computed under a few assumed limiting wall and ground responses. The results are plotted in Fig. 5 for the probabilities of exceeding the chosen limiting wall deflection ($\delta_{\mathrm{lim},hm}$) and ground settlement ($\delta_{\mathrm{lim},vm}$). The probability of exceedance is seen to decrease with the chosen limiting deformation (either wall deflection or ground settlement) which is consistent with the study by Hsiao et al. (2008). The effect of the scale of fluctuation on the probability of exceedance is clearly observed. When relatively smaller limiting $\delta_{\mathrm{lim},hm}$ and $\delta_{\mathrm{lim},vm}$ are adopted, the scenario with a smaller scale of fluctuation yields a higher probability of exceedance. The trend reverses when relatively larger limiting $\delta_{\mathrm{lim},hm}$ and $\delta_{\mathrm{lim},vm}$ are adopted. For the probability of exceeding the limiting wall deflection, the reversal of the trend occurs when $\delta_{\mathrm{lim},hm} \approx 108$ mm is adopted. Similarly, for the probability of exceeding the limiting ground settlement, the reversal of the trend occurs when $\delta_{\mathrm{lim},vm} \approx 72$ mm is adopted. Of course, this observation may not be generalized as it may be specific to the TNEC case. Further studies are needed to confirm this observation. Nevertheless, the results show that neglecting the spatial soil variability in the analysis can lead to either overestimation or underestimation of the probability of exceedance, depending on the chosen limiting wall and ground responses. Thus, it is important to assess the spatial variability in site investigation and to incorporate this variability in the probability analysis. A similar conclusion of the effect of scale of fluctuation on the probability of failure for slope stability problems was reported by Griffiths and Fenton (2004) using the rigorous random FEM approach, which shows the validity of the proposed approach.

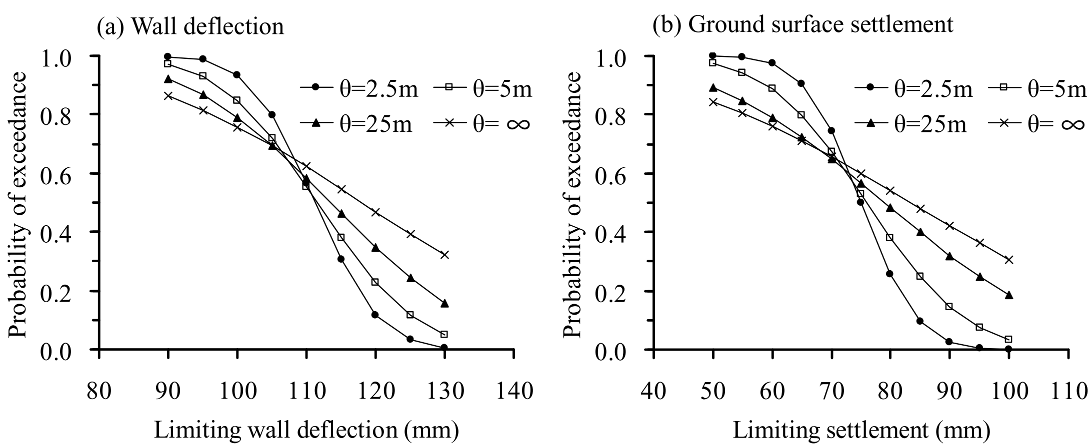

Figure 5. Computed probability of exceedance at various levels of limiting wall deflection and ground surface settlement

CONCLUSIONS

The fuzzy finite element approach (FFEA) is shown to be effective in the analysis of the wall and ground responses in a braced excavation through the study of a well-documented excavation case history. PLAXIS with the modified pseudo plasticity (MPP) soil model is found satisfactory for predicting the wall and ground responses in a braced excavation. The spatial averaging technique in the finite element analysis of the braced excavation in clays demonstrates the effect of spatial correlation of soil properties on the responses in a braced excavation. Neglecting the spatial variability in the finite element analysis can lead to either overestimation or underestimation of the probability of exceedance, depending on the specified limiting wall and ground responses.

REFERENCES

Brinkgreve, R. B. J., and Vermeer, P.A. (1998). *PLAXIS-Finite Element Code for Soil and Rocks Analysis*, Version 8, Balkema, Rotterdam.

Dang, H.P. (2009). "Excavation behavior and adjacent building response analyses using user defined soil models in PLAXIS." MS Thesis, National Taiwan University of Science and Technology, Taipei, Taiwan.

Dodagoudar, G.R., and Venkatachalam, G. (2000). "Reliability analysis of slopes using fuzzy sets theory." *Computers and Geotechnics*, 27(2), 101-115.

Dong, W.M., and Wong, F.S. (1987). "Fuzzy weighted averages and implementation of the extension principle." *Fuzzy Set and Systems*, 21(2), 183-199.

Duncan, J.M. (2000). "Factors of safety and reliability in geotechnical engineering." *Journal of Geotechnical Geoenvironmental Engineering*, 126(4), 307-316.

Griffiths, D.V., and Fenton, G.A. (2004). "Probabilistic slope stability analysis by finite elements." *Journal of Geotechnical and Geoenvironmental Engineering*, 130(5), 507-518.

Hsiao, E.C.L., Schuster, M., Juang, C.H., and Kung, T.C. (2008). "Reliability analysis of excavation-induced ground settlement for building serviceability evaluation." *Journal of Geotechnical and Geoenvironmental Engineering*, 134(10), 1448-1458.

Kung, T.C., Hsiao, C.L., and Juang, C.H. (2007). "Evaluation of a simplified small-strain soil model for finite element analysis of excavation-induced movements." *Canadian Geotechnical Journal*, 44(6), 726-736.

Ou, C.Y., Liao, J.T., and Lin, H.D. (1998). "Performance of diaphragm wall constructed using top-down method." *Journal of Geotechnical and Geoenvironmental Engineering*, 124(9), 798-808.

Peschl, G.M., and Schweiger, H.F. (2003). "Reliability analysis in geotechnics with finite elements - comparison of probabilistic, stochastic and fuzzy set methods." *In: Proceedings of the 3rd international symposium on imprecise probabilities and their applications* (ISIPTA'03), Carleton Scientific, Canada, 437-451.

Phoon, K.K., and Kulhawy, F.H. (1999). "Evaluation of geotechnical property variability." *Canadian Geotechnical Journal*, 129(4), 625-639.

Schweiger, H.F., and Peschl, G.M. (2005). "Reliability analysis in geotechnics with the random set finite method." *Computers and Geotechnics*, 32(6), 422-435.

Vanmarcke, E.H. (1977). "Probabilistic modeling of soil profiles." *Journal of the geotechnical engineering division*, 103(11), 1227-1246.

Zadeh, L.A. (1965). "Fuzzy sets." *Information and Control*, 8(3), 338-353.

Evaluation of LRFD Resistance Factors and Risk for Mechanically Stabilized Earth Walls

S. Wasman[1*], M. McVay[2], D. Bloomquist[3], M. Harrison[4], and P. Lai[5]

[1*] PhD Student, Department of Civil and Coastal Engineering, University of Florida, 365 Weil Hall, Gainesville, Fl, 32611, ph (352) 392-9537, fx (352) 392-3394, e-mail: swasman@ufl.edu
[2] Professor, Department of Civil and Coastal Engineering, University of Florida, Gainesville, Fl, e-mail: mcm@ce.ufl.edu
[3] Associate Professor, Department of Civil and Coastal Engineering, University of Florida, Gainesville, Fl, e-mail: dave@ce.ufl.edu
[4] Assistant Professor, Department of Nuclear and Radiological Engineering, University of Florida, Gainesville, Fl, e-mail: marc.harrison@ufl.edu
[5]Florida Department of Transportation, Tallahassee, Fl, e-mail: peter.lai@dot.state.fl.us

ABSTRACT

The use of Mechanically Stabilized Earth (MSE) walls is very common in congested urban areas. AASHTO's current LRFD resistance values were established from Allowable Stress Design Factors of Safety. Variability of soil friction angle, unit weight, cohesion, etc. is not considered. This study investigates the influence of soil property variability on MSE wall sliding and bearing stability and compares Capacity Demand Ratio (CDR) distributions from conventional analytical approaches with laboratory centrifuge model results. Next, the probability of failures (CDR < 1.0) and associated variability is applied in risk assessment of two MSE walls used in existing transportation infrastructure subsystems. The risk assessment was used to develop recommended probability of failures in design to meet the associated cost of repair if catastrophic failures of the walls are to occur.

INTRODUCTION

Geotechnical design codes have moved towards a reliability-based approach such as the Load and Resistance Factor Design (AASHTO, 2009) and away from Allowable Stress Design (ASD) with factors of safety. Resistance factors for all modes of failure in the code for retaining walls were developed through calibration with ASD Factors of Safety (FS). Unfortunately, the latter approach does not account for the influence of the soil properties variability on the resistance factors. Moreover, the resistance and loads calculated in a retaining wall external stability analysis are directly influenced by the soil properties. Soil variability and its influence on the stability of retaining walls has been investigated through a number of probabilistic analyses (Chalermyanont and Benson, 2005; Fenton and Griffiths, 2005; Zevgolis and Bourdeau, 2008; Babu and Basha, 2008).

This work also characterizes the variability through Monte Carlo simulations of reinforced backfill and foundation soils with rigid body mechanics using Rankine earth pressure assumptions (Chalermyanont and Benson, 2005) to establish a probability distribution of CDR (capacity demand ratio = resistance force/driving force) as a function of soil properties. Next, to identify the bias in the external stability methods, small scale centrifuge tests were performed to establish experimental CDR histograms based on soil properties (e.g. angle of internal friction angle and unit weight of backfill). Next, using a Monte Carlo bias correction similar to Goh (2008), for cantilever retaining walls, LRFD resistance values are suggested for specific probabilities of failure. Note, the fitting of the measured CDR histogram with the analytical probability distribution should provide more realistic resistance values than those proposed in AASHTO for external stability of MSE walls.

Since 90% of the retaining walls in the State of Florida are MSE with a significant portion in urban areas, a failure is potentially hazardous, depending on the mode. Therefore, a risk assessment which quantifies the probability of failure, P_f, in terms of consequence values (i.e., risk = P_f X consequence) was undertaken. Such an assessment allows for owners, engineers, contractors, etc. to identify where the risk lies and where to focus in the design to decrease the P_f and thereby the risk. The paper presents a probability risk assessment for two failure modes (sliding and bearing) with varied consequences in different settings (urban city, arterial overpass abutments, suburban areas, etc.).

PROBABILISTIC ANALYSIS

For this work, a prototype wall height of 9.1m with L/H ratio of 1.0 and surcharge load of 12 kN/m^2 was considered (Figure 1). The unit weight and friction angle were modeled as lognormal (non-negative values and accounts for possible outliers) and, conservatively, as having no correlation (Goh, 2009; Fenton and Griffiths, 2005). Mean and coefficient of variation, CV, values consistent with those

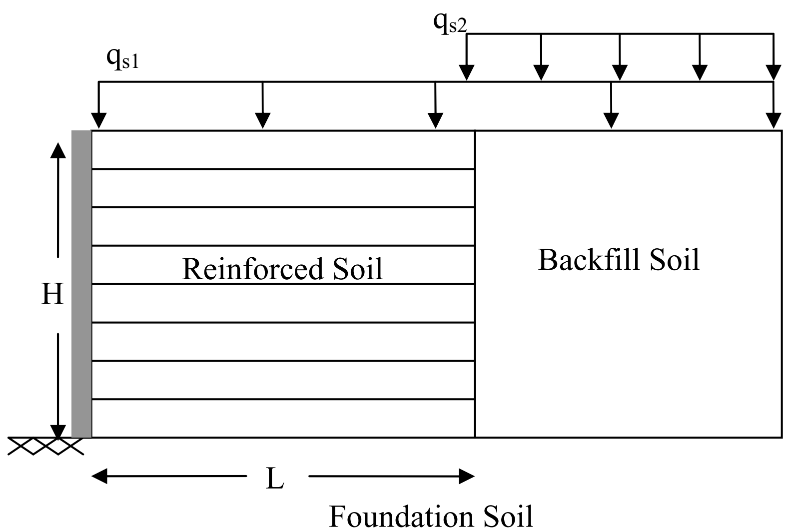

Figure 1. MSE wall with acting surcharge.

reported in research literature (Duncan, 2000; Zevgolis and Bourdeau, 2006; Fenton and Griffiths, 2008) were considered and are presented as the base model values in Table1.

The probability of failure for each mode (sliding and bearing capacity) was defined with the limit state, in terms of a Capacity Demand Ratio (CDR<1). Equations 1 and 2 show each CDR as a function of the factored driving and resisting forces and stresses. The modes of failure were considered to be independent in this study, i.e., the probabilities presented are not inducing failure in another mode. The loads and resistances were factored with values suggested in the AASHTO LRFD Bridge Design Specifications (AASHTO, 2009).

Table 1. Range of statistical parameters of soil properties and surcharge for analysis. Base model parameters shown in parenthesis.

Soil	Mean (μ)	Coefficient of Variation (CV)	Distribution
Reinforced Soil φ	20° - 40° (30°)	5% - 20% (10%)	Lognormal
Reinforced Soil γ	15kN/m^3 - 19kN/m^3 (16.5 kN/m^3)	5% - 20% (5%)	Lognormal
Backfill Soil φ	20° - 40° (30°)	5% - 20% (10%)	Lognormal
Backfill Soil γ	15 kN/m^3 - 19 kN/m^3 (16.5 kN/m^3)	5% - 20% (5%)	Lognormal
Foundation Soil φ	20° - 40° (35°)	5% - 20% (10%)	Lognormal
Foundation Soil γ	15 kN/m^3 - 19 kN/m^3 (16.5 kN/m^3)	5% - 20% (5%)	Lognormal
Surcharge q_s	12 kN/m^2	5% - 20% (25%)	Lognormal

The equations of CDR for sliding and bearing stability of an MSE wall are shown below:

$$CDR_{sliding} = \frac{F_{Resisting}}{F_{Driving}} = \frac{\gamma H Tan(\phi) \cdot \phi_g}{\frac{1}{2}\gamma H^2 K_a EH + q_s H K_a LS} \qquad \text{Eq. 1}$$

$$CDR_{bearing} = \frac{q_{ultimate}}{q_{vertical}} = \frac{(\gamma D_f N_q + \frac{1}{2}\gamma L N_\gamma)\phi_g}{\gamma HEV + q_s LS} \qquad \text{Eq. 2}$$

where $F_{Resisting}$ is the factored shear resistance at the reinforced-foundation soil interface, $F_{Driving}$ is the factored active driving force, $q_{ultimate}$ is the factored bearing capacity, and $q_{vertical}$ is the factored vertical stress at the reinforced-foundation soil interface due to the weight of the soil and the surcharge (q_{s2}).

SCALE MODEL TESTS

As part of an the ongoing study, centrifuge tests to model sliding of a 15 cm high MSE wall with length equal to height (L/H =1) were done in the 12-G Ton facility at the University of Florida. The wall modeled full scale MSE walls, i.e., to allow flexibility of the reinforced zone (Fig. 1) and with non-extensible reinforcement according to the Florida structures guidelines. Model soils used in the tests were selected to obtain internal friction angles within the ranges considered (Table 1). The model wall was 15 cm in height and had a reinforcement length equal to the height (L/H = 1). The reinforced, backfill and foundation soils were varied to obtain μ_ϕ, μ_γ, CV_ϕ and CV_γ values in the range of those in Table 1. Surcharge loading (12 kN/m^2) was modeled using a Bimba piston applied to a flexible surface for uniform contact stresses. During testing, wall displacements were monitored for vertical movement and horizontal movement near the top and bottom of the wall face. To determine the CDR of sliding, horizontal and vertical force sensors measured soil forces that contributed to the total driving (P_a) and resisting forces (τ) in the model.

Multiple tests were performed and from each test a CDR value was obtained so that a frequency distribution could be established along with distribution type and summary statistics (i.e., μ_{CDR}, CV_{CDR}). Figure 2 is a distribution of 16 centrifuge test results for sliding where the variability of the reinforced and backfill soil was held at

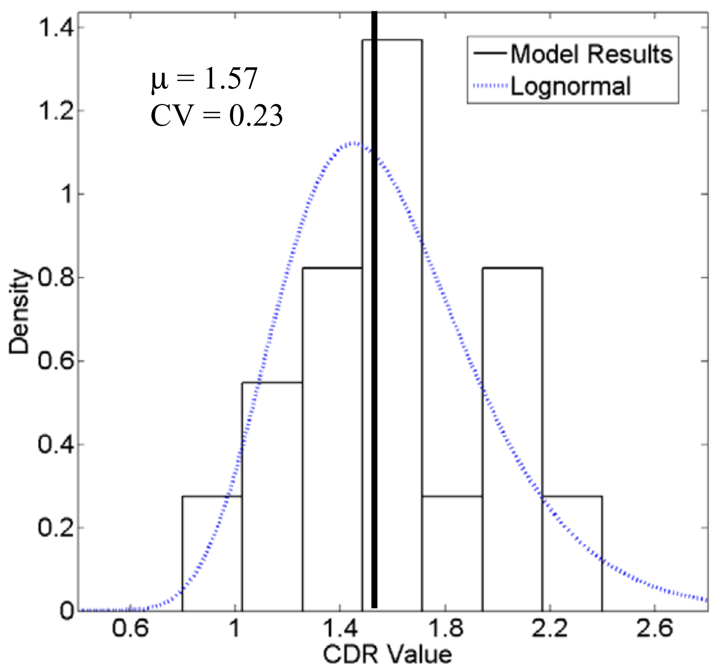

Figure 2. Distribution of centrifuge sliding model tests: μ_ϕ = 35° and CV_ϕ = 4% of reinforced and backfill soil.

μ_ϕ = 35° and CV_ϕ = 4%. Based on a fit test presented by Klammler et al. (2011) a ratio of skewness, *sk*, to CV of the model data suggests a gamma distribution. However, since the analytical expression (Eq. 1) of the CDR is lognormal, the latter was selected here, with the area under the tail i.e. CDR<1 defined as the probability of failure of interest. As suggested by Paikowksy et al. (2010), a new LRFD Φ factor for a target P_f may be found by equating the areas underneath the tails where CDR <1 between the experimental and analytical values. Also, the ratio of the P_f's for the measured (centrifuge) to predicted (analytical) should be determined for each external case considered as well as the soil variability investigated.

RISK ASSESSMENT

Risk is the probability of failure times the consequence of the failure. Geotechnical structures such as MSE walls (soil-soil interaction) have been shown to have P_f values associated with independent modes of stability. Consequences of structural failures include loss of life, economic impact, social impact, and environmental impacts with attempts at quantifying values associated with each have been made for Civil Infrastructure systems, e.g. the levee system failures in New Orleans during Hurricane Katrina (USACOE, 2007). Methods of modeling complex systems with P_f analysis consists of fault trees, event trees and master logic diagrams. They allow a logical representation of the system (e.g., MSE) in terms of the P_f and associated components. For example, a fault tree diagram for the MSE wall would have the top event as the global stability of the wall. Underneath the top event, events, or all stability modes (i.e., sliding, bearing, overturning and overall), are listed which contribute to the top events occurrence. Each mode of stability and its P_f is a component of the system and each mode also has components which are function of the soil properties (characterized by μ and CV). The result is a total P_f for the system (i.e., MSE) which can be calculated by a consequence term to obtain an associated risk value.

Risk assessments and methods for geotechnical engineering have been presented for landslides (Fell, 1994), flooding (Fenton and Griffiths, 2008), and talus slopes (Liu et al., 2009). In these studies, specific risks were assessed based on different consequences. For example, the landslide risk assessment considered the vulnerability of houses and persons, the houses having a more easily quantifiable $ value associated with damage incurred. The example of different flooding cases considered cost ($) due to repair, cost ($) to flood proof the houses and cost ($) to prevent flooding by constructing a levee. The risk assessment presented in this paper considers specific risk for the MSE wall's components P_f.

The simplest and most common value quantified is economic consequence (dollars-$), whether its cost to a region or cost of structural repair. In cases where MSE walls are part of the transportation infrastructure, a risk assessment can be made where the economic consequence is determined from the negative impact on value travel time (VTT). For instance, in transportation engineering, the incremental consumer surplus is a measure by which designers assess benefit of increased traffic lanes (Lee, 2000). Incremental consumer surplus is the area under a demand curve between the initial and improved cost to the user. In the case of MSE wall failure, the resulting economic loss of traffic lanes, may be taken as the negative of the incremental consumer surplus, or that the user will incur costs which will be reflected as a loss in the consumer surplus.

In addition to the costs incurred by the roadway users, other economic consequences can include the repair cost for the MSE wall and roadway. Repair costs are commonly the only consequence considered, as assessing other consequences are quite difficult or beyond the responsibility of the engineer.

RISK ASSESSMENT EXAMPLES

Two examples where MSE walls serve as part of the transportation infrastructure were considered for risk assessment. Site A is a two lane overpass and is a commuter artery for east and west bound traffic with the major employer in the area located 16.9 km southeast of an urban area. Site B is a US Interstate overpass with six lanes separated by a median. Each site is located in north Florida and FDOT publishes traffic data for each (FDOT, 2009). The economic consequence value used in the examples is the negative incremental consumer surplus (NICS) for an inelastic demand along with repair costs. NICS is a function of the cars per day which pass the specific location, a value travel time (VTT) based on typical values for local and interstate roads (US DOT, 1997), and the occupancy rate for the region. The estimated repair costs are per square meter of MSE wall and per kilometer of roadway (FDOT, 2010) as shown in Table 2, along with the other parameters described. The total cost value (NICS + Repairs) for each site is based on the number of traffic lanes out of service for 15 days following MSE wall failure.

Table 2. Economic consequence values for example sites (US$).

Site	Cars/day	VTT $/per./hr.	Occ. Rate Pers./car	Days	NICS ($mil)	$/m^2	$mil/km	Repairs ($mil)	Total Cost ($mil)
A	22,000	12.13	1.14	15	4.6	484	2.4	0.4	5
B	59,000	16.89	1.14	15	17	484	5.9	0.5	17.5

Maximum P_f values for sliding and bearing modes (equations 1 and 2) obtained in the Monte Carlo simulations are shown in Table 3. In a simulation, the property in each column was varied over a range while the other properties were held constant at the base model (values in parenthesis in Table 1). Each P_f was obtained from 4,000,000 realizations of CDR, the number required to ensure $CV_{Pf} < 10\%$. With the consequence values (total cost) given in Table 2, the risk specific to each parameter in Table 3 is calculated (P_f x consequence) and presented in Tables 4 and 5 in units of millions of US$.